Psychological Medicine (2017), **47**, 1609–1623. © Cambridge University Press 2017
doi:10.1017/S0033291717000058

ORIGINAL ARTICLE

Anatomical integration and rich-club connectivity in euthymic bipolar disorder

S. O'Donoghue[1]*, L. Kilmartin[2], D. O'Hora[3], L. Emsell[4], C. Langan[1], S. McInerney[5], N. J. Forde[6], A. Leemans[7], B. Jeurissen[8], G. J. Barker[9], P. McCarthy[10], D. M. Cannon[1] and C. McDonald[1]

[1] *The Centre for Neuroimaging & Cognitive Genomics (NICOG) and NCBES Galway Neuroscience Centre, National University of Ireland Galway, Galway, Republic of Ireland*
[2] *College of Engineering and Informatics, National University of Ireland Galway, Galway, Republic of Ireland*
[3] *School of Psychology, National University of Ireland Galway, Galway, Republic of Ireland*
[4] *Translational MRI, Department of Imaging & Pathology, KU Leuven & Radiology, University Hospitals Leuven, Leuven, Belgium*
[5] *Department of Psychiatry, St Michael's Hospital, Toronto, Ontario, Canada*
[6] *Department of Psychiatry, University Medical Centre Groningen, Groningen, The Netherlands*
[7] *Image Sciences Institute, University Medical Center Utrecht, Utrecht, The Netherlands*
[8] *Vision Lab, University of Antwerp, Antwerp, Belgium*
[9] *Institute of Psychiatry, Psychology and Neuroscience, London, UK*
[10] *Radiology, University Hospital Galway, Galway, Republic of Ireland*

Background. Although repeatedly associated with white matter microstructural alterations, bipolar disorder (BD) has been relatively unexplored using complex network analysis. This method combines structural and diffusion magnetic resonance imaging (MRI) to model the brain as a network and evaluate its topological properties. A group of highly interconnected high-density structures, termed the 'rich-club', represents an important network for integration of brain functioning. This study aimed to assess structural and rich-club connectivity properties in BD through graph theory analyses.

Method. We obtained structural and diffusion MRI scans from 42 euthymic patients with BD type I and 43 age- and gender-matched healthy volunteers. Weighted fractional anisotropy connections mapped between cortical and subcortical structures defined the neuroanatomical networks. Next, we examined between-group differences in features of graph properties and sub-networks.

Results. Patients exhibited significantly reduced clustering coefficient and global efficiency, compared with controls globally and regionally in frontal and occipital regions. Additionally, patients displayed weaker sub-network connectivity in distributed regions. Rich-club analysis revealed subtly reduced density in patients, which did not withstand multiple comparison correction. However, hub identification in most participants indicated differentially affected rich-club membership in the BD group, with two hubs absent when compared with controls, namely the superior frontal gyrus and thalamus.

Conclusions. This graph theory analysis presents a thorough investigation of topological features of connectivity in euthymic BD. Abnormalities of global and local measures and network components provide further neuroanatomically specific evidence for distributed dysconnectivity as a trait feature of BD.

Received 28 April 2016; Revised 29 December 2016; Accepted 4 January 2017; First published online 13 February 2017

Key words: Bipolar disorder, diffusion tensor imaging, graph theory, magnetic resonance imaging, network analysis.

Introduction

Evidence for white matter disruption from diffusion tensor imaging (DTI) and for dysconnectivity from functional magnetic resonance imaging (fMRI) suggests impaired neuronal connectivity as a potential core feature of bipolar disorder (BD) (Strakowski *et al.* 2005, 2012; Emsell & McDonald, 2009; Vederine *et al.* 2011; Houenou *et al.* 2012; Nortje *et al.* 2013; Skudlarski *et al.* 2013; Vargas *et al.* 2013; Wessa *et al.* 2014; Kumar *et al.* 2015). In particular, studies have reported white matter microstructural abnormalities in connections between prefrontal and anterior limbic structures (Versace *et al.* 2008, 2014; Benedetti *et al.* 2011) supporting neural models of impaired emotion processing and regulation in patients with BD (Phillips & Swartz, 2014).

* Address for correspondence: S. O'Donoghue, The Centre for Neuroimaging & Cognitive Genomics (NICOG) and NCBES Galway Neuroscience Centre, College of Medicine, Nursing and Health Sciences, National University of Ireland Galway, Galway, Republic of Ireland.
(Email: s.odonoghue9@nuigalway.ie)

Advanced diffusion MRI analysis techniques examine the brain *in vivo* to define parameters of neuroanatomical connectivity. Impaired structural connectivity can be assessed on a network scale using graph theory properties (Sporns *et al.* 2000). There have been few graph analysis investigations in BD, although reduced global efficiency in patients has been reported (Leow *et al.* 2013; Collin *et al.* 2016). Studies that investigated regional segregation indicate inconsistencies (Leow *et al.* 2013; Gadelkarim *et al.* 2014; Forde *et al.* 2015), which may be related to clinical heterogeneity or variation in the range of graph properties and in-house measures utilized. Therefore, further investigation into global integration and regional segregation of structural brain networks in BD is warranted.

Complex network analysis combines structural and diffusion MRI to model the brain as a neuroanatomical network and evaluate topological organization and properties of brain structure. A network at the macroscale comprises cortical and subcortical structures represented by 'nodes', and white matter connections, represented by 'edges' (Bullmore & Sporns, 2009; Rubinov & Sporns, 2010; Sporns, 2012). Following network construction, graph theory properties characterize brain integration and segregation (Bullmore & Sporns, 2009, 2012; Rubinov & Sporns, 2010). These properties include global measures quantifying whole-brain integration and connectedness, and local measures to characterize segregation: the anatomical architecture of structural inter-connectivity with nearby regions (Bullmore & Sporns, 2009; Bassett *et al.* 2011). Therefore, graph analysis extends DTI analysis of microstructural white matter to characterize patterns of organization.

Assessment of neuroanatomical sub-networks, the connectivity between several brain regions, assumes that connections belonging to the same component are highly connected (Zalesky *et al.* 2010; Meskaldji *et al.* 2011). The Network Based Statistic (NBS) tests for connectivity effects in edge weights within sub-networks. Therefore, investigation of sub-networks may identify regionally specific structural dysconnectivity in BD.

Furthermore, key hubs with a high density of interconnections, termed the rich-club, appear to play a key role integrating brain functioning and may be impaired in brain disorders (van den Heuvel & Sporns, 2011; Collin *et al.* 2013; Crossley *et al.* 2013, 2014; Sporns & Van Den Heuvel, 2013). Hubs, or nodes that are highly connected, appear to be involved in executive function, the salience network and the default mode network when the mind is at rest (van den Heuvel & Sporns, 2011; Crossley *et al.* 2013; Senden *et al.* 2014). Rich-club structures identified in healthy human brain networks include regions previously implicated in mood regulation and BD, for example the hippocampus, striatum and thalamus (Hallahan *et al.* 2011; Houenou *et al.* 2012) and their connections (Emsell *et al.* 2013*a*, *b*; Nortje et al. *2013*; Ellison-Wright *et al.* 2014).

Previously, we demonstrated fractional anisotropy (FA) reductions in the corpus callosum and limbic pathways (Emsell *et al.* 2013*b*) that were consistent with other DTI studies (Vederine *et al.* 2011; Nortje *et al.* 2013). Therefore, we sought to further examine regional connections defined by nodes connecting the corpus callosum and cingulum (Emsell *et al.* 2013*a*). Sub-network and rich-club analysis techniques were employed to probe inter-connectivity within neural circuits potentially implicated in BD. The present study aimed to investigate dysconnectivity in BD through global, local, network component and rich-club connectivity measures in a large clinically homogeneous sample of patients with euthymic BD.

Method

Participants

A total of 42 participants with BD were included for this graph theory analysis. Of these participants with BD, 35 between 18 and 60 years of age were recruited from the local community as part of the Galway Bipolar Study (Emsell *et al.* 2013*a*, *b*). An additional seven individuals with remitted BD who participated in a follow-up imaging of a first-episode psychosis study and underwent an identical scanning procedure were included in connectivity analysis (Scanlon *et al.* 2014; Kenney *et al.* 2015). Next, we recruited 43 age- and gender-matched healthy volunteers from the local community. The 42 patients with BD type I were confirmed using the Diagnostic and Statistical Manual of Mental Disorders, 4th edition (DSM-IV) Structured Clinical Interview for DSM Disorders (American Psychiatric Association, 1994). Exclusion criteria for all participants included a history of medical or neurological illness, history of head injury resulting in loss of consciousness for over 5 min, history of substance abuse in the past year, learning disability, and oral steroid use in previous 3 months. Further exclusion criteria for controls included personal or family history of psychotic or affective disorder in first- or second-degree relatives. Additional patient exclusion criteria included a lifetime co-morbid DSM-IV Axis I disorder. All patients were euthymic at the time of scanning, defined as a score <7 on both the Hamilton Rating Scale for Depression and Young Mania Rating Scale (Hamilton, 1960; Young *et al.* 1978). Ethical approval was obtained from the National University of Ireland Galway and

https://doi.org/10.1017/S0033291717000058 Published online by Cambridge University Press

University Hospital Galway research ethics committees. After a complete description of the study was presented to participants, written informed consent was obtained.

MRI acquisition

All participants were scanned with identical imaging acquisition parameters. Structural MRI data were acquired on a 1.5 Tesla Siemens Magneto Symphony Scanner using a four-channel head coil. A volumetric T1-weighted magnetization prepared acquisition of gradient echo (MPRAGE) sequence was acquired with the imaging parameters: repetition time 1140 ms; echo time 4.38 ms; inversion time 600 ms; flip angle 15; matrix size 256 × 256; an in-plane pixel size 0.9 × 0.9 mm^2; slice thickness of 0.9 mm.

Diffusion MRI data were acquired using an eight-channel head coil with an echo planar image diffusion sequence acquired with parallel imaging, 64 optimized diffusion gradient directions with $b = 1300$ s/mm^2, seven non-diffusion weighted images, repetition time = 8100 ms, echo time = 95 ms, field of view = 240 × 240 mm^2, matrix = 96 × 96, in-plane voxel size of 2.5 × 2.5 mm^2, slice thickness = 2.5 mm, 60 slices.

Pre-processing

All MR images were corrected for subject motion and eddy current distortions using the diffusion MRI analysis software toolbox *ExploreDTI* v.4.8.3 (Leemans *et al.* 2009). The b-matrix was rotated to preserve diffusion orientation information within voxels during subject motion correction (Leemans & Jones, 2009). Quality assessment for all diffusion MR images examined scans for potential artifacts including hypointensities, shift in images, and signal dropout. We rated MR images on a quality scale from mild to severe. Participants with poor MR image quality were excluded from subsequent analyses.

Whole-brain tractography

Whole-brain white matter tractography reconstructed the series of streamlines used to define the 'edges' in complex network analysis. White matter pathways were reconstructed using *ExploreDTI* v.4.8.3 (Leemans *et al.* 2009). Robust estimation of the diffusion tensor was implemented using the RESTORE approach (Chang *et al.* 2005). A deterministic constrained spherical deconvolution algorithm accounted for crossing fibres present within voxels (Tournier *et al.* 2007; Jeurissen *et al.* 2011). Fibre tracking initiated in each voxel and continued with a step size of 1 mm until the following threshold was exceeded: fibre orientation distribution >0.15, angle threshold curvature >30°, minimum length <20 mm, and maximum length >300 mm. A spherical harmonic order of $L_{max} = 8$ was applied.

Generating connectivity matrices

The series of tractography streamlines were mapped through cortical and subcortical structures to produce a weighted and undirected 90 × 90 connectivity matrix for each subject. Connectome maps did not correct for changes in region-of-interest structural volume. Visual inspection using MRIcron confirmed registration of the cortical parcellation atlas to T1 images (Rorden *et al.* 2007).

Selection of nodes

The Automated Anatomical Labeling (AAL) Atlas parcellated cortical and subcortical volumes into 90 regions (Tzourio-Mazoyer *et al.* 2002). The AAL Atlas is a macro-anatomical parcellation atlas based on a single-subject brain template set in Montreal Neurological Institute space (Tzourio-Mazoyer *et al.* 2002). The AAL Atlas applies spatial coordinates and associated volume for 90–120 cortical and subcortical structures. Node definition excluded the cerebellum resulting in a 90-node parcellation scheme (45 nodes bilaterally).

Selection of edges

Analysis of undirected and weighted edges included streamline count between nodes and mean FA between nodes. Averaged FA values between two nodes defined the FA edge weight (Levitt *et al.* 2012). To extend the previous DTI study that reported widespread FA reductions, we implemented FA edge weights in graph theory and sub-network analysis. Additionally, analysis of rich-club connections employed streamline count edge weights to examine effects of nodes rich in connections. Streamline count represents the total number of reconstructed streamlines interconnecting two nodes. Additionally, graph thresholding was applied to remove spurious streamlines, which when unaccounted for lead to unintended false positives. Connection matrices were thresholded at a density value 0.2, which resulted in equivalent connection densities between groups but allowed connection weights to vary, minimizing false-positive streamline count (Fornito *et al.* 2012).

Network metrics

The Brain Connectivity Toolbox contains the set of functions used to produce graph theory measures (Rubinov & Sporns, 2010). Graph theory analysis implemented weighted undirected edge strengths

https://doi.org/10.1017/S0033291717000058 Published online by Cambridge University Press

across all analyses. Global and regional measures probe properties of integration and segregation (Bullmore & Sporns, 2009, 2012; Rubinov & Sporns, 2010). The metrics selected for analysis in the study are described in Table 1.

Nodal analyses were selected *a priori* from a previous DTI analysis in this cohort (Emsell *et al.* 2013*a*, *b*). Nine bilateral nodes were selected (listed in Table 3) as endpoints of prefrontal white matter, cingulum and callosal splenium connections (Emsell *et al.* 2013*a*).

NBS

Collectively impaired interconnections or sub-networks investigated with the NBS toolbox characterize network differences by identification of particular inter-regional connections or components affected in one group of individuals relative to another. Studies investigating sub-networks in a number of brain disorders applied NBS analysis; however this technique has yet to be investigated in BD (Zalesky *et al.* 2010, 2012). The NBS identifies an experimental effect at the cluster level by performing mass univariate testing controlling for family-wise error rate. First, statistical significance threshold was selected at $p < 0.05$. Next, permutation testing performed 5000 permutations. The NBS requires selection of supra-threshold connections: as this threshold setting is quite arbitrary, investigation across three supra-threshold values was employed, as has been most commonly implemented (Zalesky *et al.* 2010, 2012). Finally, all connected components' supra-threshold was compared between groups (Zalesky *et al.* 2010).

Rich-club coefficient

Next, we carried out an exploratory investigation of the 'rich-club' coefficient among cortico-subcortical connections. The 'rich-club' refers to a set of nodes that are rich in connections and densely interconnected among themselves forming a club (McAuley *et al.* 2007; van den Heuvel & Sporns, 2011). We investigated weighted rich-club connectivity differences between groups, as well as rich-club structural membership. The rich-club coefficient is defined by the following equation:

$$\phi(k) = \frac{2E > k}{N > k(N > k - 1)}$$

where by, $E > k$ indicates the weighted number of streamline connections greater than k present within a subgraph degree $>k$, as $N > k$ indicates the number of nodes in the subgraph (McAuley *et al.* 2007; Collin *et al.* 2013). The measure ϕ reflects the level of interconnectivity between nodes. The rich-club identifies structural connections with a high value of k, removing all lower-degree connections. The rich-club nodes will have a high k and high ϕ (McAuley *et al.* 2007; van den Heuvel & Sporns, 2011; Collin *et al.* 2014).

Table 1. *Weighted graph properties investigated in this study*

Weighted graph properties	Definition
Weighted degree	The number of connections attached through a node
Weighted clustering coefficient	The number of connections between a node and its connected neighbouring nodes proportionally related to the possible number of connections
Weighted characteristic path length	The average shortest path length, i.e. the minimum number of edges that must be traversed to go from one node to another
Weighted global efficiency	The inverse of the shortest path length
Weighted local efficiency	The length of the shortest path between two nodes, containing only neighbours of the node of interest
Weighted betweenness centrality	The number of shortest paths between two nodes passing through one node. Nodes that participate in many short paths reflect a node's influence in a network

Normalized rich-club coefficient

A normalized rich-club coefficient indicates that these densely interconnected structures were connected based on more than chance alone. A normalized coefficient is adjusted to a number of comparable random networks by preserving the degree distribution (van den Heuvel & Sporns, 2011). Normalized rich-club analysis uses a number of rewiring iterations of the preserved degree distribution to ensure that effects are not due to chance. The weighted normalized rich-club coefficient is given by the following equation:

$$\phi w_{norm}(k) = \frac{\phi w(k)}{\phi w_{random}(k)}$$

A weighted normalized rich-club coefficient $\Phi w_{\mathrm{norm}}(k)$ was computed as the weighted rich-club parameter $\Phi w(k)$ over a set of $m = 500$ random networks of equal degree. As the sufficient number of rewirings lacks standardization with re-arrangements (m) ranging from 100 to 1000 (van den Heuvel & Sporns, 2011; Daianu *et al.* 2015; Kocher *et al.* 2015), selection of a number of random rewirings ($m = 500$) revealed a

https://doi.org/10.1017/S0033291717000058 Published online by Cambridge University Press

standard deviation that converges below 0.001. The number of appropriate rewiring iterations ($m = 500$) was set at 10 to ensure that normalization was met. By definition, $\Phi w_{norm} > 1$ over a range of k implies the existence of a rich-club set (McAuley *et al.* 2007; van den Heuvel & Sporns, 2011).

Rich-club membership

Validation methods confirmed rich-club membership. Rich-club members defined at the statistical significant network between patients and controls ($k = 56$) displayed approximately 10–12 highly connected nodes. We identified rich-club members at $\Phi w_{norm} > 1$ across range k at a group threshold of 60 and 70% of participants to determine rich-club structures most consistent across individual networks. Additionally, the top 10 highest weighted degree nodes confirmed that rich-club members were not dependent on one hub definition alone.

Statistics

Statistical analysis of global and regional metrics (degree, clustering coefficient, betweenness centrality, characteristic path length, global efficiency and local efficiency) applied multivariate analysis of covariance tests, co-varied for age and gender, using IBM SPSS statistics software version 22 (IBM SPSS Amos, 2012). Calculations of global values from nodal measures averaged values across all 90 nodes to generate a global average for each measure. We corrected for global connectivity to assess whether findings were indicative of reduced connectivity globally or potentially affected topological organization. Global analyses and regional comparisons underwent false discovery rate (FDR) correction for multiple comparisons (Benjamini & Hochberg, 1995).

Permutation testing was used to assess between-group effects in rich-club connectivity. We performed 9999 Monte Carlo resamples using R software (RStudio Team, 2012). Multiple comparisons corrected for 28 possible values of k density were implemented using the FDR method (Benjamini & Hochberg, 1995).

We applied partial correlations co-varying for age and gender to assess the relationship between clinical symptoms scales, illness duration and lithium use, and significant graph theory metrics. Global efficiency was correlated with rich-club density co-varying for age and gender to determine a possible relationship between global integration and hub inter-connectivity.

Results

The sociodemographic and clinical details of the participants are outlined in Table 2. Participants and healthy volunteers were age and gender matched. On average, patients had a lower number of years of education than healthy volunteers. The mean age of onset of illness in patients was 28 years of age. Of the patients, 33 took mood stabilizers at the time of scanning, with most using lithium (29); 22 patients took antipsychotics, with most using olanzapine (15); and eight patients used antidepressants. Four participants in the BD group were unmedicated at the time of the MRI scan.

Global and regional graph theory metrics

Analysis of global properties revealed statistically significant group differences whereby the BD group displayed increased characteristic path length and reduced global efficiency and clustering coefficient compared with the healthy volunteer group when connections were weighted by FA (Fig. 1 and online Supplementary Table S1). Seven of the regions connected by fronto-limbic and parieto-occipital pathways revealed significantly reduced connectivity surviving multiple comparison correction. In BD, reduced clustering and local efficiency predominantly incorporated the superior and middle frontal nodes and superior and middle occipital nodes, when defined by FA (Table 3). Findings did not change when corrected for global connectivity, defined by the global density metric. Preserved measures of degree and density indicate that significant differences in topology may be the primary feature of BD.

NBS

The BD group displayed significantly weaker subnetwork connectivity, with a single dysconnected subnetwork identified for each threshold (2, 2.5, 3). The NBS provides two outputs: (*a*) the supra-threshold set of connections comprised in the graph component found to show a significant effect; as well as (*b*) a corresponding p value for each such network (Zalesky *et al.* 2010) (Fig. 2). We identified collective network dysconnectivity differences with supra-threshold connections ($t = 2$, $p = 0.015$), consisting of frontal, parietal and occipital connections in BD. Higher supra-threshold connections ($t = 2.5$, $p = 0.017$; and $t = 3$, $p = 0.020$) revealed structural dysconnectivity among parietal and occipital connections in patients compared with healthy controls.

Rich-club connectivity

In this analysis, rich-club organization was evident across a range of connection densities. The weighted rich-club connection density ranged from 27 to 64 possible densities, while the normalized weighted rich-club

https://doi.org/10.1017/S0033291717000058 Published online by Cambridge University Press

Table 2. *Clinical and demographic variables*[a]

	Healthy controls	Bipolar group	Statistical comparison: test statistic, p
Number of subjects	43	42	
Age, years	40.3 (9.5)	39.3 (10.3)	$t = 1.497$, $p = 0.138$
Gender, n			$\chi^2 = 0.110$, $p = 0.740$
Male	20	23	
Female	22	19	
Education, years	17.9 (2.9)	15.4 (3.6)	$t = 3.329$, $p < 0.001$
Age of onset, years	–	28.7 (7.9)	
Illness duration, years	–	10.9 (8.8)	
Number of hospitalizations	–	1.5 (1)	
Hamilton Depression Rating Scale	–	0.9 (1.4)	
Range		0–7	
Young Mania Rating Scale	–	0.45 (1)	
Range		0–4	
Global Assessment of Functioning	–	84.5 (5.3)	

Data are given as mean (standard deviation) unless otherwise indicated.

[a] Participants were age and gender matched. Years of education differed between groups. All participants in the bipolar group were confirmed prospectively euthymic with clinical rating scales of mania and depression less than a score of 7.

Table 3. Regional connectivity differences between patients and controls[a]

Nodes		Clustering coefficient F (p)	Local efficiency F (p)
Precentral gyrus	Left	2.641 (0.108)	3.415 (0.068)
	Right	5.078 (0.027)	7.819 (0.006)
Superior frontal gyrus	Left	6.575 (0.012)	9.411 (0.003*)
	Right	0.049 (0.825)	4.147 (0.045)
Middle frontal gyrus	Left	5.464 (0.022)	10.937 (0.001*)
	Right	3.174 (0.079)	8.271 (0.005*)
Medial superior frontal gyrus	Left	6.422 (0.013)	5.042 (0.027)
	Right	4.323 (0.041)	5.499 (0.021)
Anterior cingulate gyrus	Left	6.402 (0.013)	4.897 (0.030)
	Right	4.978 (0.028)	4.30 (0.040)
Middle cingulate gyrus	Left	0.654 (0.421)	2.415 (0.124)
	Right	1.818 (0.181)	5.084 (0.027)
Superior parietal gyrus	Left	2.955 (0.089)	3.400 (0.069)
	Right	5.258 (0.024)	3.786 (0.055)
Superior occipital gyrus	Left	15.371 (0.000*)	12.913 (0.001*)
	Right	6.929 (0.010)	9.870 (0.002*)
Middle occipital gyrus	Left	6.185 (0.015)	8.527 (0.005*)
	Right	4.669 (0.034)	5.097 (0.027)

[a] This analysis examined two different local graph measures in fractional anisotropy connections. Multivariate analyses of covariance were carried out between groups, co-varying for age and gender. Nine nodes bilaterally were selected *a priori* from a previous data-driven diffusion tensor imaging analysis (Emsell *et al.* 2013*a*, *b*) for analyses of local graph theory measures.

* Significant p value after false discovery rate correction.

coefficient ranged from 28 to 56. The group comparison of normalized weighted rich-club connectivity effects demonstrated statistically significant differences before FDR multiple comparison correction across two possible connection densities ($k = 55$, $Z = -2.236$, $p = 0.024$; $k = 56$, $Z = -2.654$, $p = 0.0067$). After FDR correction for 28 possible densities, the highest density ($k = 56$) demonstrated a moderate to large effect size (Cohen's $d = 0.59$).

https://doi.org/10.1017/S0033291717000058 Published online by Cambridge University Press

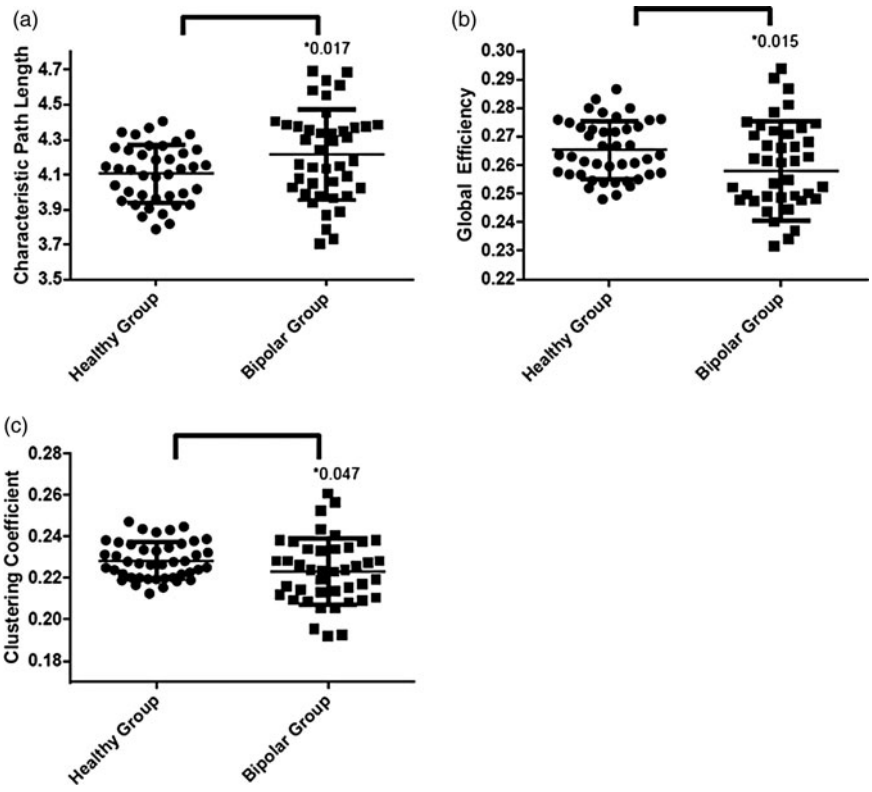

Fig. 1. Global metrics defined by fractional anisotropy connection weight in bipolar disorder patients and controls show unadjusted values for (*a*) characteristic path length, (*b*) global efficiency and (*c*) clustering coefficient. The mean is represented by the middle line, with bars representing standard error.

Rich-club membership

Following examination of rich-club connectivity effects, we investigated rich-club membership. Rich-club structures were selected by the group-averaged cortico-subcortical network for the statistically significant $\Phi w_{\mathrm{norm}}(k)$ and identified nodes connected by this pathway. Rich-club connections shared by 60% of participants indicate differential hub participation between groups. Although we identified rich-club members connected by pathways at the 60% group threshold, we applied a more stringent threshold of 70% to identify what findings were consistent. Previously, pathways present in >50% of participants were taken into account (van den Heuvel & Sporns, 2011). Additionally, the top 10 highest degree nodes were identified to validate the threshold selection (van den Heuvel & Sporns, 2011; Collin *et al.* 2014).

Rich-club members revealed the following hubs: superior frontal gyrus, middle cingulate gyrus, hippocampus, caudate, precuneus and thalamus (Fig. 3). In BD, rich-club membership at the group threshold of 60% indicated that the right frontal superior gyrus and right middle cingulate gyrus were not included in the rich-club in most BD patients; however, BD rich-club structures incorporate the left middle occipital gyrus. Of interest, when we assessed rich-club membership in 70% of participants, the most notable between-group differences in the BD group supported the absence of the right superior frontal gyrus and left thalamus as hubs, and additionally the left middle occipital gyrus was no longer integrated in patients (Fig. 3). Of note, dysconnections identified by the NBS analysis overlap with rich-club members, namely the left hippocampus, precuneus and thalamus.

Partial correlations show that rich-club connectivity is associated with global efficiency in all participants ($r = 0.299$, $p < 0.006$) (online Supplementary Fig. S1). Taken together, the normalized rich-club coefficient revealed trend connectivity effects as well as rich-club membership differences. Global efficiency appears to be related to rich-club connectivity, supporting the role of rich-club connections in global integration.

Clinical associations

Partial correlations did not reveal any significant association between graph theory properties and the clinical measures assessed: age of onset, illness duration, whether patients were taking lithium at the time of scan or had previously taken lithium, and years of medication use.

https://doi.org/10.1017/S0033291717000058 Published online by Cambridge University Press

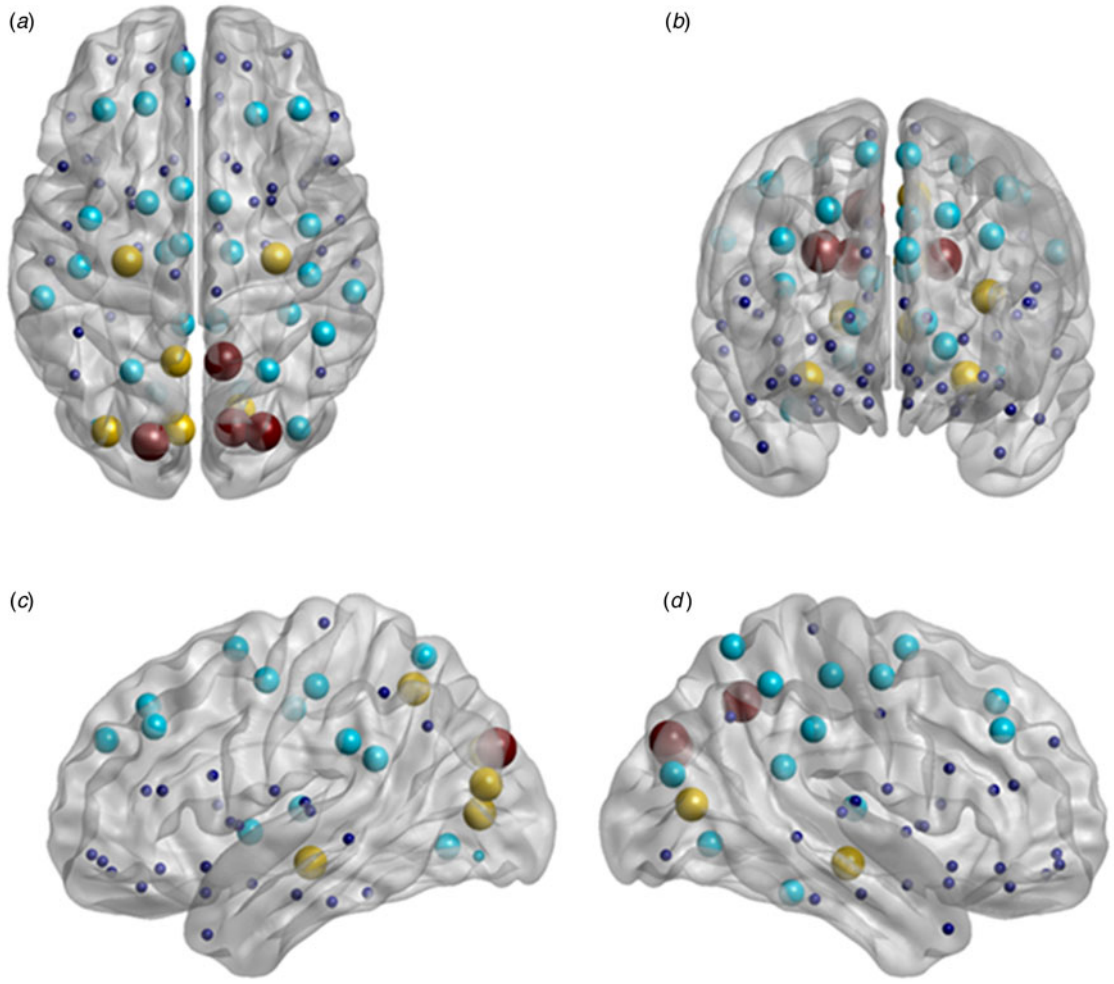

Fig. 2. Density of nodal connections in participant groups determined by network-based statistic (NBS) analysis. Nodal alterations identified in NBS toolbox, with colour and size of sphere indicating increasing *t*-statistic thresholds. Dark blue nodes indicate Automated Anatomical Labeling (AAL) nodes which did not significantly differ at any threshold. Light blue nodes ($T = 2$) identify a reduction in density of connections in the bipolar disorder (BD) group compared with the control group. Similarly, yellow nodes ($T = 2.5$) and red nodes ($T = 3$) represent reduced density of connections in the BD group at higher thresholds. (*a*) Axial orientation; (*b*) coronal orientation; (*c*) left sagittal orientation; (*d*) right sagittal orientation.

Discussion

This study provides novel evidence of distributed neuroanatomical dysconnectivity, using a range of graph theory metrics, as a trait-based feature of BD. In summary, we identified disrupted anatomical integration and regional segregation in fronto-limbic and posterior parietal regions and reduced inter-connection density of sub-networks that converged among posterior parietal circuits in the BD group compared with healthy volunteers. We also demonstrated absence of rich-club structures in BD, most consistently the right superior frontal gyrus. Therefore, this study confirms disrupted global anatomical integration and represents the first study to show impaired frontal hub integration using graph analysis in BD.

This investigation is consistent with three studies that identified reduced global efficiency in BD (Leow *et al.* 2013; Gadelkarim *et al.* 2014; Collin *et al.* 2016). However, two other studies determined connectivity to be preserved globally (Forde *et al.* 2015; Wheeler *et al.* 2015). Potential differences in results between the current investigation and other studies may be due to the parcellation scheme employed. In contrast to the present analysis which used volumetric parcellation, one study used cortical thickness to define nodes and did not demonstrate differences in connection density between healthy individuals and BD in a multi-centre study (Wheeler *et al.* 2015). Furthermore, in contrast with the investigation by Forde *et al.* (2015) that weighted connections by streamline count,

https://doi.org/10.1017/S0033291717000058 Published online by Cambridge University Press

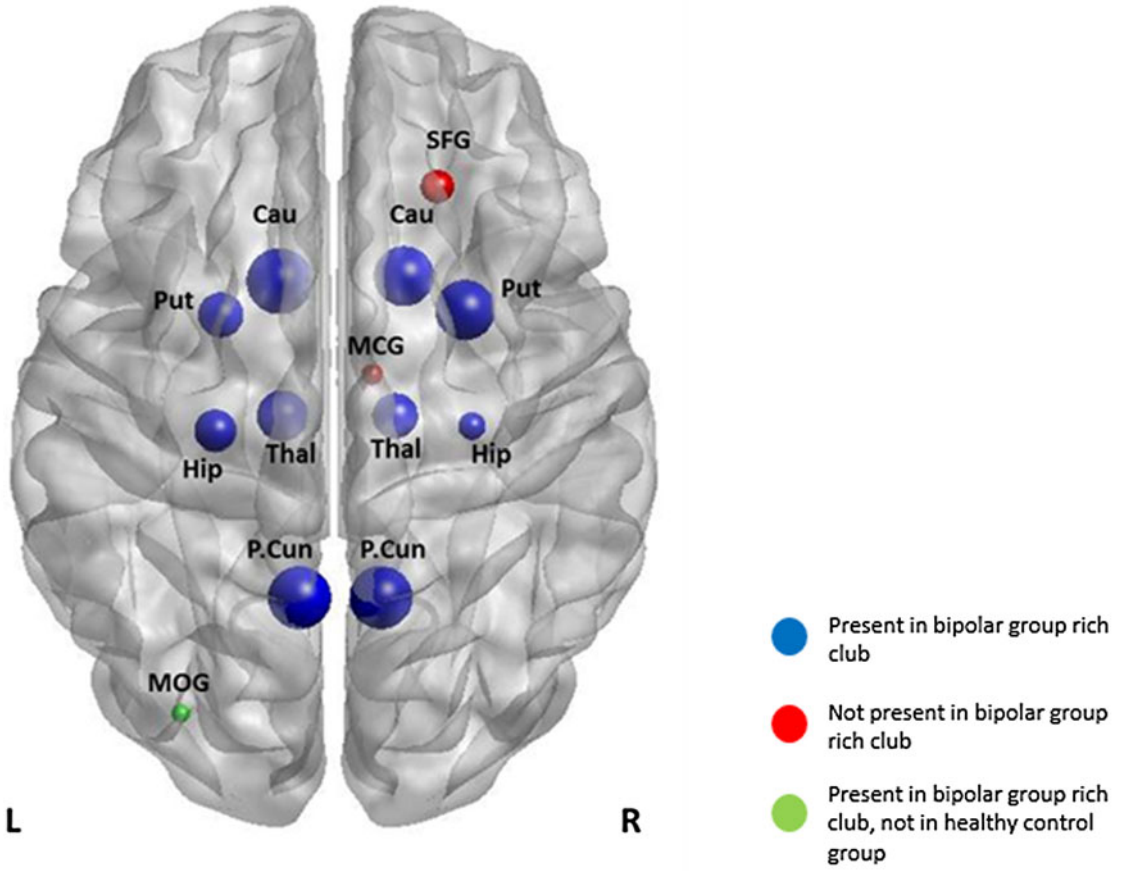

Fig. 3. Rich-club membership in patients and controls. Rich-club membership in the participants with differences between groups colour coded. All nodes presented represent rich-club members common to all healthy volunteers, while nodes in red indicate structures absent in the rich-club in the bipolar group, i.e. right superior frontal gyrus (SFG) and left thalamus (Thal). Nodes in green represent rich-club structures recruited in the bipolar group, not present in the healthy control group. Size of sphere relates to rich-club structures common to 60% of participants, larger spheres common to 95–100% of participants. Cau, Caudate; Put, putamen; MCG, middle cingulate gyrus; Hip, hippocampus; P.Cun, precuneus; MOG, middle occipital gyrus; L, left; R, right.

we identified reductions in global efficiency and average clustering coefficient when connections were weighted by FA. Impaired global integration may be a general pathophysiological feature across brain disorders (Crossley *et al.* 2014; Fornito *et al.* 2015); therefore, regional connectivity may elucidate topological patterns involved in emotional dysregulation and its effect on whole-brain integration.

Uncorrected regional analyses of clustering and local efficiency identified widespread reductions among fronto-limbic, parietal and occipital connections, consistent with previous studies (Leow *et al.* 2013; Gadelkarim *et al.* 2014; Forde *et al.* 2015). Furthermore, regional dysconnectivity of the left middle frontal gyrus and right superior medial frontal gyrus has been supported in a recent investigation in patients from families multiply affected with BD (Forde *et al.* 2015). Similarly, the present dataset demonstrates callosal dysconnectivity due to regional frontal patterns of disorganization. Additionally, parietal and default mode network dysconnectivity identified by regional and network-based analysis is corroborated by an investigation of path length-associated community estimation (Gadelkarim *et al.* 2014). This analysis indicates that connectivity abnormalities in BD appear to extend beyond fronto-limbic regions to other association areas of the brain (Vederine *et al.* 2011; Nortje *et al.* 2013; Wise *et al.* 2016). These reductions may be related to features of topological dysconnectivity as opposed to reduced connectivity globally, as findings were unchanged when corrected for global connectivity.

Furthermore, the NBS measure identified a collection of interconnections encompassing fronto-limbic and parietal/occipital connections (Gadelkarim *et al.* 2014). Moreover, weaker connectivity of network components in patients indicates that these impaired connections interact collectively, supporting BD as a

https://doi.org/10.1017/S0033291717000058 Published online by Cambridge University Press

dysconnection syndrome (O'Donoghue *et al.* 2015). Analysis of highest supra-threshold connections revealed dysconnectivity among the cuneus, precuneus and superior occipital connections. Interestingly, evidence from functional connectivity analyses supports a model of an affected posterior default mode network as well as parieto-occipital dysconnectivity (Strakowski *et al*. 2005, 2011). Strakowski *et al.* (2000, 2002) proposed that self-referential thinking and interpretation of visual stimuli are affected in disturbances of this network, namely altered functional connectivity of the precuneus and cuneus. These structures are topologically central with high degree, which may be particularly affected in BD (Crossley *et al.* 2014; Gadelkarim *et al.* 2014).

Investigation of rich-club connectivity effects shows trend-level reductions in BD. The associated relationship between global efficiency and rich-club density suggests that widespread neuroanatomical dysconnectivity may be related to communication among these central structures (van den Heuvel *et al.* 2013; Crossley *et al.* 2014). Recent studies report reduced rich-club connectivity in schizophrenia and unaffected siblings with schizophrenia (van den Heuvel *et al.* 2013; Collin *et al.* 2014, 2016). In BD, one study to date has reported preserved rich-club connections (Collin *et al.* 2016). Results of the present cortico-subcortical rich-club connectivity analysis are in contrast to this study which was confined to cortico-cortical connections (Collin *et al.* 2016). The significance of the limbic system in BD argues for the inclusion of subcortical limbic structures in network mapping. Differences in subcortical volume in BD has a substantial body of literature to support its role in the aetiology and as a trait feature of the illness (Houenou *et al.* 2012; Strakowski *et al.* 2012; Vargas *et al*. 2013; Quigley *et al.* 2015; Hibar *et al.* 2016; van Erp *et al.* 2016). Additionally, during tract reconstruction we implemented constrained spherical deconvolution to overcome the challenges of white matter reconstruction in subcortical areas.

Next, we address the consistency in rich-club structures and hubs affected in BD. Therefore, this investigation examined regions connected by the statistically significant pathway and detected hub involvement specific to BD. The investigation by Collin *et al.* (2016) examined additional rich-club classifications using the top 20% betweenness-centrality nodes and top 10% highest degree nodes. These hubs consisted of portions of the bilateral cingulate, precuneus, superior frontal, parietal and temporal gyri, as well as pre- and post-central gyri and insular cortices (Collin *et al.* 2016). In the present study, we defined hubs connecting pathways present in most participants and validated by top 10% highest degree nodes, which confirmed these rich-club structures. Cingulate, precuneus and superior frontal structures appear to be consistent across investigations and hub definitions, potentially due to above-average connectivity and participation across both cortical and cortico-subcortical mappings (van den Heuvel *et al.* 2013; Collin *et al.* 2014, 2016). Additionally, rich-club members in this analysis were identified as hubs in a study of patients with schizophrenia, defined by betweenness centrality, when network analysis implemented the equivalent structural atlas (van den Heuvel *et al.* 2010). Validation of this parcellation scheme merits reproducibility of these structures as critical hubs in cortico-subcortical networks.

In the current study, the superior frontal gyrus was absent from the BD group rich-club, suggesting differential involvement of this densely interconnected frontal structure. Hub deficits reported in a study of patients with schizophrenia support rich-club members affected in the current analysis, consistent with a less central role of frontal hubs in psychotic illnesses (van den Heuvel *et al.* 2010). This absence was maintained when the rich-club pathway was defined among group thresholds of 60% of patients and 70% of patients. Models of neural circuitry in BD suggest that decreased grey matter volume and aberrant functional connectivity in the right ventrolateral prefrontal cortex are features of impaired emotional processing and regulation in BD (Phillips & Swartz, 2014). Nodes anatomically connected with the superior frontal gyrus, also present in the rich-club network, include the caudate and thalamus (Haznedar *et al.* 2005; Li *et al.* 2013). These deficits are consistent with a DTI study reporting reduced FA in the anterior thalamic radiation in both BD and schizophrenia patients (Sussmann *et al.* 2009). While thalamic function has been implicated previously in BD, volumetric analyses of the thalamus have been varied (Hallahan *et al.* 2011). Rich-club members presented in the 60% group threshold indicated above-average connectivity of the right middle cingulate gyrus in healthy controls, absent in the BD group. Moreover, the BD group rich-club additionally involves the left middle occipital gyrus, which may potentially represent a compensatory effect from disrupted frontal connectivity (Griffa *et al.* 2013). Differential involvement of rich-club structures and reduced connection density between these rich-club structures may well contribute to the global connectivity effects identified in this study.

Reduced local efficiency in prefrontal regions, anterior cingulate cortex, and absence of the superior frontal gyrus as a rich-club hub is consistent with impaired top-down connectivity of prefrontal and ventral–limbic emotional circuits as suggested by Strakowski *et al.* (2012) and Phillips & Swartz (2014). Aberrant

https://doi.org/10.1017/S0033291717000058 Published online by Cambridge University Press

connectivity of the amygdala was not identified in this study, although it has been considered a characteristic marker underlying emotional dysregulation (Strakowski *et al.* 2012). Some reports have shown that amygdala activity and volume 'normalize' when patients are in remission (Hallahan *et al.* 2011; Phillips & Swartz, 2014) and may account for the lack of significant dysconnectivity of this important limbic node. This investigation extends current models of BD with evidence of more widespread and posterior abnormalities, suggesting that dysconnectivity extends beyond these prefrontal networks. Notably, a meta-analysis of DTI studies in BD also suggests that posterior white matter dysconnectivity may be related to impaired cognitive functioning that persists in patients with BD (Nortje *et al.* 2013).

Inter-hemispheric dysconnectivity was not specifically examined in this investigation, where it has been supported as a feature of BD in previous structural network studies (Leow *et al.* 2013; Caeyenberghs & Leemans, 2014; Gadelkarim *et al.* 2014; Collin *et al.* 2016).

Methodological selections must be considered when interpreting these network findings (de Reus & van den Heuvel, 2013; Fornito *et al.* 2013). As network analyses lack standardized recommendations and methodological criteria at this point; this network reconstruction carries challenges when interpreting and reconciling results across investigations (Fornito *et al.* 2013). Methodological considerations in this novel and evolving field include the specific choice of parameters for white matter tract reconstruction, crossing fibres, edge weights of FA measures and streamline count. Advancing from previous research by use of more biologically relevant connection weights as well as a template cortical parcellation may identify less variable effects (Fornito *et al.* 2013). The AAL template employs an identical cortico-subcortical parcellation atlas for each participant; therefore, subject-specific cortical and subcortical volume changes were not accounted for in this analysis. Subject-specific parcellation schemes have their own inconsistencies, e.g. FreeSurfer-generated nodes may be implemented with or without manual correction of the boundaries of subcortical segmentation (McCarthy *et al.* 2015). Extension of this work would improve from a subject-specific parcellation technique integrated in network analysis reliably. The field would benefit from some degree of standardization in these approaches, which would assist in directly comparing results as they emerge from research groups.

A strength of the current analysis is the parcellation scheme employed in the brain mapping pipeline. A majority of complex network analyses limit their connectome maps to cortical connection maps, while this analysis extended to cortico-subcortical mapping. The scale at which the brain should be accurately mapped to be most biologically meaningful is not yet standardized (Fornito *et al.* 2013). Additionally, we attempt to explain hub participation differences in BD through examination of rich-club membership. The heterogeneity of network analysis techniques and graph properties available makes comparison between studies and meta-analyses challenging. The present investigation utilized certain commonly employed graph metrics, such as global efficiency and clustering coefficient, in order to facilitate comparison of our results with those of other studies. These graph properties were selected as they specifically quantify a node's influence in network integration and segregation. In addition, certain more novel metrics, involving sub-network and rich-club connectivity, were employed given their recent application to other disorders and the convergent evidence for regional neuroanatomical dysconnectivity as a core feature of BD.

Taken together, these analytical methods support previous DTI investigations, and extend further understanding of structural dysconnectivity in BD. The relationship of graph measures to pathophysiological mechanisms is an active area of examination (Fornito *et al.* 2013). The relevance of this study indicates dysconnectivity to be a pathophysiologically relevant trait-related feature of BD, with differentially affected rich-club structures being particularly informative to describe complex structural integration.

Conclusion

This multifaceted analysis employing graph theory metrics provides substantial additional evidence for anatomical dysconnectivity representing a trait feature of BD. This study supports reductions in global efficiency and local connectedness of limbic structures, and extends initial investigations of BD sub-networks, identifying weaker connected components incorporating anterior and posterior brain networks representing trait features of BD.

Supplementary material

The supplementary material for this article can be found at https://doi.org/10.1017/S0033291717000058

Acknowledgements

This research was supported by the Hardiman Research Scholarship, National University of Ireland, Galway, Galway Ireland and the Health Research Board (HRA_POR/2011/100). We gratefully acknowledge the

participants of this study and the radiographers of the University Hospital Galway Magnetic Resonance Imaging Department for their support during data collection.

The research of A.L. is supported by VIDI grant 639.072.411 from the Netherlands Organization for Scientific Research (NWO). B.J. is a postdoctoral fellow supported by the Research Foundation Flanders (FWO Vlaanderen). G.J.B. receives honoraria for teaching from General Electric Healthcare, and acts as a consultant for IXICO.

Declaration of Interest

None.

References

American Psychiatric Association (1994). *Diagnostic and Statistical Manual of Mental Disorders*, 4th edn. APA: Washington, DC.

Bassett DS, Brown JA, Deshpande V, Carlson JM, Grafton ST (2011). Conserved and variable architecture of human white matter connectivity. *NeuroImage* **54**, 1262–1279.

Benedetti F, Absinta M, Rocca MA, Radaelli D, Poletti S, Bernasconi A, Dallaspezia S, Pagani E, Falini A, Copetti M, Colombo C, Comi G, Smeraldi E, Filippi M (2011). Tract-specific white matter structural disruption in patients with bipolar disorder. *Bipolar Disorders* **13**, 414–424.

Benjamini Y, Hochberg Y (1995). Controlling the false discovery rate: a practical and powerful approach to multiple testing. *Journal of the Royal Statistical Society. Series B (Methodological)* **57**, 289–300.

Bullmore E, Sporns O (2009). Complex brain networks: graph theoretical analysis of structural and functional systems. *Nature Reviews. Neuroscience* **10**, 186–198.

Bullmore E, Sporns O (2012). The economy of brain network organization. *Nature Reviews. Neuroscience* **13**, 336–349.

Caeyenberghs K, Leemans A (2014). Hemispheric lateralization of topological organization in structural brain networks. *Human Brain Mapping* **35**, 4944–4957.

Chang LC, Jones DK, Pierpaoli C (2005). RESTORE: Robust Estimation of Tensors by Outlier Rejection. *Magnetic Resonance in Medicine* **53**, 1088–1095.

Collin G, Kahn RS, De Reus MA, Cahn W, Van Den Heuvel MP (2014). Impaired rich club connectivity in unaffected siblings of schizophrenia patients. *Schizophrenia Bulletin* **40**, 438–448.

Collin G, Sporns O, Mandl RCW, Van Den Heuvel MP (2013). Structural and functional aspects relating to cost and benefit of rich club organization in the human cerebral cortex. *Cerebral Cortex* **24**, 2258–2267.

Collin G, van den Heuvel MP, Abramovic L, Vreeker A, de Reus MA, van Haren NEM, Boks MPM, Ophoff RA, Kahn RS (2016). Brain network analysis reveals affected connectome structure in bipolar I disorder. *Human Brain Mapping* **37**, 122–134.

Crossley NA, Mechelli A, Scott J, Carletti F, Fox PT, McGuire P, Bullmore ET (2014). The hubs of the human connectome are generally implicated in the anatomy of brain disorders. *Brain* **137**, 2382–2395.

Crossley NA, Mechelli A, Vértes PE, Winton-Brown TT, Patel AX, Ginestet CE, McGuire P, Bullmore ET, Vertes PE, Winton-Brown TT, Patel AX, Ginestet CE, McGuire P, Bullmore ET (2013). Cognitive relevance of the community structure of the human brain functional coactivation network. *Proceedings of the National Academy of Sciences of the United States of America* **110**, 11583–11588.

Daianu M, Jahanshad N, Nir TM, Jack CR, Weiner MW, Bernstein MA, Thompson PM (2015). Rich club analysis in the Alzheimer's disease connectome reveals a relatively undisturbed structural core network. *Human Brain Mapping* **36**, 3087–3103.

de Reus MA, van den Heuvel MP (2013). The parcellation-based connectome: limitations and extensions. *NeuroImage* **80**, 397–404.

Ellison-Wright I, Nathan PJ, Bullmore ET, Zaman R, Dudas RB, Agius M, Fernandez-Egea E, Müller U, Dodds CM, Forde NJ, Scanlon C, Leemans A, McDonald C, Cannon DM (2014). Distribution of tract deficits in schizophrenia. *BMC Psychiatry* **14**, 99.

Emsell L, Langan C, Van Hecke W, Barker GJ, Leemans A, Sunaert S, McCarthy P, Nolan R, Cannon DM, McDonald C (2013*a*). White matter differences in euthymic bipolar I disorder: a combined magnetic resonance imaging and diffusion tensor imaging voxel-based study. *Bipolar Disorders* **15**, 365–376.

Emsell L, Leemans A, Langan C, Van Hecke W, Barker GJ, McCarthy P, Jeurissen B, Sijbers J, Sunaert S, Cannon DM, McDonald C (2013*b*). Limbic and callosal white matter changes in euthymic bipolar I disorder: an advanced diffusion magnetic resonance imaging tractography study. *Biological Psychiatry* **73**, 194–201.

Emsell L, McDonald C (2009). The structural neuroimaging of bipolar disorder. *International Review of Psychiatry (Abingdon, England)* **21**, 297–313.

Forde NJ, O'Donoghue S, Scanlon C, Emsell L, Chaddock C, Leemans A, Jeurissen B, Barker GJ, Cannon DM, Murray RM, McDonald C (2015). Structural brain network analysis in families multiply affected with bipolar I disorder. *Psychiatry Research – Neuroimaging* **234**, 44–51.

Fornito A, Zalesky A, Breakspear M (2013). Graph analysis of the human connectome: promise, progress, and pitfalls. *NeuroImage* **80**, 426–444.

Fornito A, Zalesky A, Breakspear M (2015). The connectomics of brain disorders. *Nature Reviews. Neuroscience* **16**, 159–172.

Fornito A, Zalesky A, Pantelis C, Bullmore ET (2012). Schizophrenia, neuroimaging and connectomics. *NeuroImage* **62**, 2296–2314.

Gadelkarim JJ, Ajilore O, Schonfeld D, Zhan L, Thompson PM, Feusner JD, Kumar A, Altshuler LL, Leow AD (2014). Investigating brain community structure abnormalities in bipolar disorder using path length associated community estimation. *Human Brain Mapping* **35**, 2253–2264.

Griffa A, Baumann PS, Thiran JP, Hagmann P (2013). Structural connectomics in brain diseases. *NeuroImage* **80**, 515–526.

Hallahan B, Newell J, Soares JC, Brambilla P, Strakowski SM, Fleck DE, Kieseppä T, Altshuler LL, Fornito A, Malhi GS, McIntosh AM, Yurgelun-Todd DA, Labar KS, Sharma V, MacQueen GM, Murray RM, McDonald C (2011). Structural magnetic resonance imaging in bipolar disorder: an international collaborative mega-analysis of individual adult patient data. *Biological Psychiatry* **69**, 326–335.

Hamilton M (1960). A rating scale for depression. *Journal of Neurology, Neurosurgery and Psychiatry* **23**, 56–62.

Haznedar MM, Roversi F, Pallanti S, Baldini-Rossi N, Schnur DB, Licalzi EM, Tang C, Hof PR, Hollander E, Buchsbaum MS (2005). Fronto-thalamo-striatal gray and white matter volumes and anisotropy of their connections in bipolar spectrum illnesses. *Biological Psychiatry* **57**, 733–742.

Hibar DP, Westlye LT, van Erp TGM, Rasmussen J, Leonardo CD, Faskowitz J, Haukvik UK, Hartberg CB, Doan NT, Agartz I, Dale AM, Gruber O, Krämer B, Trost S, Liberg B, Abé C, Ekman CJ, Ingvar M, Landén M, Fears SC, Freimer NB, Bearden CE, Sprooten E, Glahn DC, Pearlson GD, Emsell L, Kenney J, Scanlon C, McDonald C, Cannon DM, Almeida J, Versace A, Caseras X, Lawrence NS, Phillips ML, Dima D, Delvecchio G, Frangou S, Satterthwaite TD, Wolf D, Houenou J, Henry C, Malt UF, Bøen E, Elvsåshagen T, Young AH, Lloyd AJ, Goodwin GM, MacKay CE, Bourne C, Bilderbeck A, Abramovic L, Boks MP, van Haren NEM, Ophoff RA, Kahn RS, Bauer M, Pfennig A, Alda M, Hajek T, Mwangi B, Soares JC, Nickson T, Dimitrova R, Sussmann JE, Hagenaars S, Whalley HC, McIntosh AM, Thompson PM, Andreassen OA (2016). Subcortical volumetric abnormalities in bipolar disorder. *Molecular Psychiatry* **21**, 1710–1716.

Houenou J, d'Albis M-A, Vederine F-E, Henry C, Leboyer M, Wessa M (2012). Neuroimaging biomarkers in bipolar disorder. *Frontiers in Bioscience* (*Elite edition*) **4**, 593–606.

IBM SPSS Amos (2012). IBM SPSS Amos. *IBM Software Business Analytics*, YTD03114-U, 1–8.

Jeurissen B, Leemans A, Jones DK, Tournier J-D, Sijbers J (2011). Probabilistic fiber tracking using the residual bootstrap with constrained spherical deconvolution. *Human Brain Mapping* **32**, 461–479.

Kenney J, Anderson-Schmidt H, Scanlon C, Arndt S, Scherz E, McInerney S, McFarland J, Byrne F, Ahmed M, Donohoe G, Hallahan B, McDonald C, Cannon DM (2015). Cognitive course in first-episode psychosis and clinical correlates: a 4 year longitudinal study using the MATRICS Consensus Cognitive Battery. *Schizophrenia Research* **169**, 101–108.

Kocher M, Gleichgerrcht E, Nesland T, Rorden C, Fridriksson J, Spampinato MV, Bonilha L (2015). Individual variability in the anatomical distribution of nodes participating in rich club structural networks. *Frontiers in Neural Circuits* **9**, 16.

Kumar J, Iwabuchi S, Oowise S, Balain V, Palaniyappan L, Liddle PF (2015). Shared white-matter dysconnectivity in schizophrenia and bipolar disorder with psychosis. *Psychological Medicine* **45**, 759–770.

Leemans A, Jeurissen B, Sijbers J, Jones DK (2009). ExploreDTI: a graphical toolbox for processing, analyzing, and visualizing diffusion MR data. In *Proceedings of the 17th Scientific Meeting, International Society for Magnetic Resonance in Medicine*, 3537 (http://cds.ismrm.org/protected/09MProceedings/files/1_program.htm).

Leemans A, Jones DK (2009). The B-matrix must be rotated when correcting for subject motion in DTI data. *Magnetic Resonance in Medicine* **61**, 1336–1349.

Leow A, Ajilore O, Zhan L, Arienzo D, GadElkarim J, Zhang A, Moody T, Van Horn J, Feusner J, Kumar A, Thompson P, Altshuler L (2013). Impaired inter-hemispheric integration in bipolar disorder revealed with brain network analyses. *Biological Psychiatry* **73**, 183–193.

Levitt JJ, Alvarado JL, Nestor PG, Rosow L, Pelavin PE, McCarley RW, Kubicki M, Shenton ME (2012). Fractional anisotropy and radial diffusivity: diffusion measures of white matter abnormalities in the anterior limb of the internal capsule in schizophrenia. *Schizophrenia Research* **136**, 55–62.

Li W, Qin W, Liu H, Fan L, Wang J, Jiang T, Yu C (2013). Subregions of the human superior frontal gyrus and their connections. *NeuroImage* **78**, 46–58.

McAuley JJ, da Fontoura Costa L, Caetano TS (2007). Rich-club phenomenon across complex network hierarchies. *Applied Physics Letters* **91**, 84103.

McCarthy CS, Ramprashad A, Thompson C, Botti J-A, Coman IL, Kates WR (2015). A comparison of FreeSurfer-generated data with and without manual intervention. *Frontiers in Neuroscience* **9**, 379.

Meskaldji DE, Ottet MC, Cammoun L, Hagmann P, Meuli R, Eliez S, Thiran JP, Morgenthaler S (2011). Adaptive strategy for the statistical analysis of connectomes. *PLoS ONE* **6**, e23009.

Nortje G, Stein DJ, Radua J, Mataix-Cols D, Horn N (2013). Systematic review and voxel-based meta-analysis of diffusion tensor imaging studies in bipolar disorder. *Journal of Affective Disorders* **150**, 192–200.

O'Donoghue S, Cannon DM, Perlini C, Brambilla P, McDonald C (2015). Applying neuroimaging to detect neuroanatomical dysconnectivity in psychosis. *Epidemiology and Psychiatric Sciences* **24**, 298–302.

Phillips ML, Swartz HA (2014). A critical appraisal of neuroimaging studies of bipolar disorder: toward a new conceptualization of underlying neural circuitry and a road map for future research. *American Journal of Psychiatry* **171**, 829–843.

Quigley SJ, Scanlon C, Kilmartin L, Emsell L, Langan C, Hallahan B, Murray M, Waters C, Waldron M, Hehir S, Casey H, McDermott E, Ridge J, Kenney J, Donoghue SO, Nannery R, Ambati S, McCarthy P, Barker GJ, Cannon DM (2015). Psychiatry research : neuroimaging volume and shape analysis of subcortical brain structures and ventricles in euthymic bipolar I disorder. *Psychiatry Research: Neuroimaging* **233**, 324–330.

Rorden C, Karnath H-O, Bonilha L (2007). Improving lesion–symptom mapping. *Journal of Cognitive Neuroscience* **19**, 1081–1088.

RStudio Team (2012). RStudio: integrated development environment for R. RStudio, Inc.: Boston, MA (http://www.rstudio.com/).

Rubinov M, Sporns O (2010). Complex network measures of brain connectivity: uses and interpretations. *NeuroImage* **52**, 1059–1069.

Scanlon C, Anderson-Schmidt H, Kilmartin L, McInerney S, Kenney J, McFarland J, Waldron M, Ambati S, Fullard A, Logan S, Hallahan B, Barker GJ, Elliott MA, McCarthy P, Cannon DM, McDonald C (2014). Cortical thinning and caudate abnormalities in first episode psychosis and their association with clinical outcome. *Schizophrenia Research* **159**, 36–42.

Senden M, Deco G, De Reus MA, Goebel R, Van Den Heuvel MP (2014). Rich club organization supports a diverse set of functional network configurations. *NeuroImage* **96**, 174–182.

Skudlarski P, Schretlen DJ, Thaker GK, Stevens MC, Keshavan MS, Sweeney JA, Tamminga CA, Clementz BA, O'Neil K, Pearlson GD (2013). Diffusion tensor imaging white matter endophenotypes in patients with schizophrenia or psychotic bipolar disorder and their relatives. *American Journal of Psychiatry* **170**, 886–898.

Sporns O (2012). From simple graphs to the connectome: networks in neuroimaging. *NeuroImage* **62**, 881–886.

Sporns O, Tononi G, Edelman GM (2000). Connectivity and complexity: the relationship between neuroanatomy and brain dynamics. *Neural Networks : the Official Journal of the International Neural Network Society* **13**, 909–922.

Sporns O, Van Den Heuvel MP (2013). Network maps of the human brain's rich club. *Network Science* **1**, 248–250.

Strakowski SM, Adler CM, DelBello MP (2002). Volumetric MRI studies of mood disorders: do they distinguish unipolar and bipolar disorder? *Bipolar Disorders* **4**, 80–88.

Strakowski SM, DelBello MP, Adler C, Cecil DM, Sax KW (2000). Neuroimaging in bipolar disorder. *Bipolar Disorders* **2**, 148–164.

Strakowski SM, Delbello MP, Adler CM (2005). The functional neuroanatomy of bipolar disorder: a review of neuroimaging findings. *Molecular Psychiatry* **10**, 105–116.

Strakowski SM, Eliassen JC, Lamy M, Cerullo MA, Allendorfer JB, Madore M, Lee JH, Welge JA, Delbello MP, Fleck DE, Adler CM (2011). Functional magnetic resonance imaging brain activation in bipolar mania: evidence for disruption of the ventrolateral prefrontal–amygdala emotional pathway. *Biological Psychiatry* **69**, 381–388.

Strakowski SSM, Adler CMC, Almeida J, Altshuler LL, Blumberg HP, Chang KD, DelBello MP, Frangou S, McIntosh A, Phillips ML, Sussman JE, Townsend JD (2012). The functional neuroanatomy of bipolar disorder: a consensus model. *Bipolar Disorders* **14**, 313–325.

Sussmann JE, Lymer GK, McKirdy J, Moorhead TW, Muñoz Maniega S, Job D, Hall J, Bastin ME, Johnstone EC, Lawrie SM, McIntosh AM (2009). White matter abnormalities in bipolar disorder and schizophrenia detected using diffusion tensor magnetic resonance imaging. *Bipolar Disorders* **11**, 11–18.

Tournier JD, Calamante F, Connelly A (2007). Robust determination of the fibre orientation distribution in diffusion MRI: non-negativity constrained super-resolved spherical deconvolution. *NeuroImage* **35**, 1459–1472.

Tzourio-Mazoyer N, Landeau B, Papathanassiou D, Crivello F, Etard O, Delcroix N, Mazoyer B, Joliot M (2002). Automated anatomical labeling of activations in SPM using a macroscopic anatomical parcellation of the MNI MRI single-subject brain. *NeuroImage* **15**, 273–289.

van den Heuvel MP, Mandl RCW, Stam CJ, Kahn RS, Hulshoff Pol HE (2010). Aberrant frontal and temporal complex network structure in schizophrenia: a graph theoretical analysis. *Journal of Neuroscience: the Official Journal of the Society for Neuroscience* **30**, 15915–15926.

van den Heuvel MP, Sporns O (2011). Rich-club organization of the human connectome. *Journal of Neuroscience: the Official Journal of the Society for Neuroscience* **31**, 15775–15786.

van den Heuvel MP, Sporns O, Collin G, Scheewe T, Mandl RCW, Cahn W, Goñi J, Hulshoff Pol HE, Kahn RS (2013). Abnormal rich club organization and functional brain dynamics in schizophrenia. *JAMA Psychiatry* **70**, 783–792.

van Erp TGM, Hibar DP, Rasmussen JM, Glahn DC, Pearlson GD, Andreassen OA, Agartz I, Westlye LT, Haukvik UK, Dale AM, Melle I, Hartberg CB, Gruber O, Kraemer B, Zilles D, Donohoe G, Kelly S, McDonald C, Morris DW, Cannon DM, Corvin A, Machielsen MWJ, Koenders L, de Haan L, Veltman DJ, Satterthwaite TD, Wolf DH, Gur RC, Gur RE, Potkin SG, Mathalon DH, Mueller BA, Preda A, Macciardi F, Ehrlich S, Walton E, Hass J, Calhoun VD, Bockholt HJ, Sponheim SR, Shoemaker JM, van Haren NEM, Pol HEH, Ophoff RA, Kahn RS, Roiz-Santiañez R, Crespo-Facorro B, Wang L, Alpert KI, Jönsson EG, Dimitrova R, Bois C, Whalley HC, McIntosh AM, Lawrie SM, Hashimoto R, Thompson PM, Turner JA (2016). Subcortical brain volume abnormalities in 2028 individuals with schizophrenia and 2540 healthy controls via the ENIGMA consortium. *Molecular Psychiatry* **21**, 547–553.

Vargas C, López-Jaramillo C, Vieta E (2013). A systematic literature review of resting state network-functional MRI in bipolar disorder. *Journal of Affective Disorders* **150**, 727–735.

Vederine F-E, Wessa M, Leboyer M, Houenou J (2011). A meta-analysis of whole-brain diffusion tensor imaging studies in bipolar disorder. *Progress in Neuro-Psychopharmacology and Biological Psychiatry* **35**, 1820–1826.

Versace A, Almeida JRC, Hassel S, Walsh ND, Novelli M, Klein CR, Kupfer DJ, Phillips ML (2008). Elevated left and reduced right orbitomedial prefrontal fractional anisotropy in adults with bipolar disorder revealed by tract-based spatial statistics. *Archives of General Psychiatry* **65**, 1041–1052.

Versace A, Andreazza AC, Young LT, Fournier JC, Almeida JRC, Stiffler RS, Lockovich JC, Aslam HA, Pollock MH, Park H, Nimgaonkar VL, Kupfer DJ, Phillips ML (2014). Elevated serum measures of lipid peroxidation and abnormal prefrontal white matter in euthymic bipolar adults: toward peripheral biomarkers of bipolar disorder. *Molecular Psychiatry* **19**, 200–208.

Wessa M, Kanske P, Linke J (2014). Bipolar disorder: a neural network perspective on a disorder of emotion and motivation. *Restorative Neurology and Neuroscience* **32**, 51–62.

Wheeler AL, Wessa M, Szeszko PR, Foussias G, Chakravarty MM, Lerch JP, DeRosse P, Remington G, Mulsant BH, Linke J, Malhotra AK, Voineskos AN (2015). Further neuroimaging evidence for the deficit subtype of schizophrenia. *JAMA Psychiatry* **72**, 446–455.

Wise T, Radua J, Nortje G, Cleare AJ, Young AH, Arnone D (2016). Voxel-based meta-analytical evidence of structural disconnectivity in major depression and bipolar disorder. *Biological Psychiatry* **79**, 293–302.

Young RC, Biggs JT, Ziegler VE, Meyer DA (1978). A rating scale for mania: reliability, validity and sensitivity. *British Journal of Psychiatry* **133**, 429–435.

Zalesky A, Cocchi L, Fornito A, Murray MM, Bullmore E (2012). Connectivity differences in brain networks. *NeuroImage* **60**, 1055–1062.

Zalesky A, Fornito A, Bullmore ET (2010). Network-based statistic: identifying differences in brain networks. *NeuroImage* **53**, 1197–1207.

https://doi.org/10.1017/S0033291717000058 Published online by Cambridge University Press